

The Full Multi: An Open-Source, Multispecies, Multisize, Multimedia Framework for Modelling the Fate of Plastic Particles in Aquatic Systems

Prado Domercq^a, Antonia Praetorius^b and Matthew MacLeod^a

a - Department of Environmental Science, Stockholm University, Stockholm, Sweden.

b - Institute for Biodiversity and Ecosystem Dynamics, University of Amsterdam, Netherlands.

ORCID

Prado Domercq: <https://orcid.org/0000-0003-2971-5758> ; prado.domercq@aces.su.se

Antonia Praetorius: <https://orcid.org/0000-0003-0197-0116> ; a.praetorius@uva.nl

Matthew MacLeod: <https://orcid.org/0000-0003-2562-7339> ; Matthew.MacLeod@aces.su.se

ABSTRACT

We present an open-source modelling framework to explore environmental fate and transport of plastic particles in aquatic systems. The “Full Multi” models 1) fragmentation of plastic into a predefined set of size classes, 2) speciation of plastic particles between pristine, heteroaggregated, biofouled, and biofouled & heteroaggregated species, 3) dynamic vertical exchange between water layers and sediment of a freshwater system, and 4) horizontal particle transport by eddy diffusion and advective flow. The Full Multi framework relates emission rates and intrinsic properties of plastic particles and variable environmental system properties, to environmental exposure concentrations. The model can be applied to analyse scenarios with different process descriptions, plastic types, emission routes and environmental parameters for hypothesis generation, to identify dominant fate processes, and in hazard and risk assessment. Here, we illustrate the framework by modelling plastic particles with a range of densities in a generic flowing river system.

KEYWORDS

Plastic pollution; Environmental fate modelling; Freshwater; Microplastics; Open source

SOFTWARE AVAILABILITY

The model presented in this paper, The Full Multi, has been developed in Python programming language. It is freely available at https://github.com/Nano2PlastProject/TheFullMulti_RIVER. The documentation of the model together with a guided example in the form of editable Jupyter Notebooks for each of the three scenarios presented (i.e. PE, PA and PVC) are provided in the Github repository including a guide for users in the README.

1. INTRODUCTION

Plastic pollution is found in rivers, lakes and the ocean globally (Peng et al. 2020; MacLeod et al. 2021; Seville et al. 2015; González-Fernández et al. 2021). Plastic debris in aquatic systems is subject to weathering by ultraviolet light, biodegradation and physical stress that results in fragmentation and chemical degradation over time. At the same time, plastic particles can aggregate with suspended particulate matter (SPM) and can be subject to colonization by biofilms. All of these processes affect fate, transport and size distribution of plastic particles, and are likely important for determining their environmental exposure levels (Wagner et al. 2014; Horton et al. 2017; Rochman et al. 2019; Kooi and Koelmans 2019). For example, plastics with lower density than water might be transported long distances by surface currents, but the same material may sink into sediments and become immobile if it is colonized by a dense biofilm (Lobelle et al. 2021; Hoellein et al. 2019; Semcesen and Wells 2021; Kaiser, Kowalski, and Waniek 2017; Fazey and Ryan 2016; Ye and Andrady 1991). Large plastic particles that are more dense than water will sink into sediment, however fibres and small fragments of plastic with the same density may remain suspended in water due to slow settling velocities. Changes in the size, shape and effective density of plastic particles over time due to fragmentation, biofouling and formation of aggregates with natural SPM can thus strongly affect the fate and transport of plastic in the environment (Horton et al. 2017).

Despite increasing research interest in plastic in the environment, many questions remain about the processes that determine the fate and transport of plastic, and its distribution between the water column, water surface and sediments. These open questions limit our ability to forecast exposure concentrations for different plastic types and emission scenarios, and to assess potential risks. One of the key challenges is to decipher how the different fate and transport processes compete with each other under different environmental conditions and for different plastic types, so that dominant environmental fate pathways can be identified and targeted for study (Horton et al. 2017).

Even in the face of high uncertainties about appropriate process descriptions, experience with models of the fate and transport of chemicals in the environment demonstrates that models have the potential to serve as a platform to integrate information and understanding about the behaviour of plastic in the environment, and to support hypothesis generation to guide research (MacLeod et al. 2010). Once confidence has been established in a model, it can be used as a basis for formulating monitoring strategies, and to estimate environmental concentrations for risk assessment when monitoring data is limited or unavailable. In recent years modelling approaches have been developed for quantifying the export of plastics into the oceans (Siegfried et al. 2017; van Wijnen, Ragas, and Kroeze 2019; L. C. M. Lebreton et al. 2017), for assessing the processes that transport or retain plastics in rivers and river catchments areas

(Siegfried et al. 2017; Unice et al. 2019; 2019; Besseling et al. 2017), and to study the fate of plastic in the ocean (Sebille et al. 2015; L. C.-M. Lebreton, Greer, and Borrero 2012; Liubartseva et al. 2016; Koelmans et al. 2017).

The study of nanoparticles in the environment inspired the creation of multimedia mass balance fate and transport models (Praetorius, Scheringer, and Hungerbühler 2012a; Meesters et al. 2014; Garner, Suh, and Keller 2017; Liu and Cohen 2014), that have the potential to be adapted to integrate processes descriptions relevant for plastic using the same principles of nonequilibrium colloidal behaviour (Praetorius et al. 2014; Hüffer et al. 2017). Multimedia mass balance models have a modular design that permits adaptation to different regional environments, and flexibility to describe different spatial and temporal scales (MacLeod et al. 2010). In the fast evolving field of plastic pollution research, where high uncertainties exist for many process descriptions and new knowledge is constantly being generated (Jahnke et al. 2017; Arp et al. 2021), a flexible and adaptable model framework that the scientific community has free access to as open-source software fills a research need.

Here, we present an open-source, flexible multimedia mass-balance fate and transport modelling framework for plastic particles in aquatic environments. The Full Multi framework is based on a generic modular unit cell that includes first-order kinetic process descriptions for vertical transport, fragmentation, biofouling and heteroaggregation of plastic particles with natural SPM in aquatic systems. The framework can be readily parameterized to describe rivers, lakes or ocean areas at different spatial resolutions and temporal scales. The base version of the Full Multi framework can be extended with new process descriptions or by adding new mass balance compartments as new findings on plastic particle fate processes become available by modifying the mass-balance equations as described in the Full Multi repository user's manual. The aim is to provide a modelling framework that serves as a standard reference for evaluating the fate of plastic particles using easy-to-run and open access code. The framework is coded in Python and the version described in this paper is accessible via the GitHub repository https://github.com/Nano2PlastProject/TheFullMulti_RIVER.

We illustrate the Full Multi framework by application to describe three types of plastic particles with a range of densities (d); polyethylene (PE, $d=980\text{kg/m}^3$), polyamide (PA, $d=999\text{kg/m}^3$) and polyvinyl chloride (PVC, $d=1580\text{kg/m}^3$) in a generic flowing river system. The model scenarios reported in this paper can be replicated using tutorials presented as Jupyter notebooks on the Full-Multi GitHub repository (i.e. FullMulti_RiverModel_Paper_PE.ipynb, FullMulti_RiverModel_Paper_PA.ipynb and FullMulti_RiverModel_Paper_PVC.ipynb).

2. THE FULL MULTI MODEL FRAMEWORK

2.1. Model description

The Full Multi model framework's name reflects that it is a multimedia mass-balance model that tracks plastic particles in multiple sizes and multiple speciation forms. Environmental compartments within each unit cell of a Full Multi model are represented as well-mixed boxes and particle size and species-specific transport and fate processes within and between compartments are described using first order kinetics. Some process descriptions in the Full Multi model are taken from the environmental fate and transport model for (inorganic) nanoparticles developed by Praetorius et al. (Praetorius et al. 2012), and additional processes relevant to plastic particles, including fragmentation and biofouling, have been added based on a literature review. The overall mass balance is defined by a system of coupled first-order differential equations. In the default parameterization of the framework described in this paper there are five particle size classes (i.e. 0.1, 1, 10, 100 and 1000 μm particles) and four speciation states (i.e. pristine, heteroaggregated, biofouled, and biofouled & heteroaggregated), thus for each compartment in the modeled system there are ($5 \times 4 =$) 20 coupled mass balance equations.

2.1.1. The unit cell and the model domain

Models of plastic transport and fate in aquatic systems are built up in the Full Multi framework by connecting two different types of environmental compartment: water and sediment. Compartments are linked to define model unit cells, and unit cells are linked to define the entire modeled domain. The default unit cell of the Full Multi model consists of three water compartments and one sediment compartment (Figure 1). As applied to describe a generic river system in the default parameterization, the compartments represent: (1) surface water, (2) flowing water, (3) stagnant water and (4) surface sediment, however their properties (Table 1) and connectivity can be adjusted to represent other aquatic systems (e.g. a unit cell representing a lake or several interconnected cells via eddy diffusion representing the global ocean).

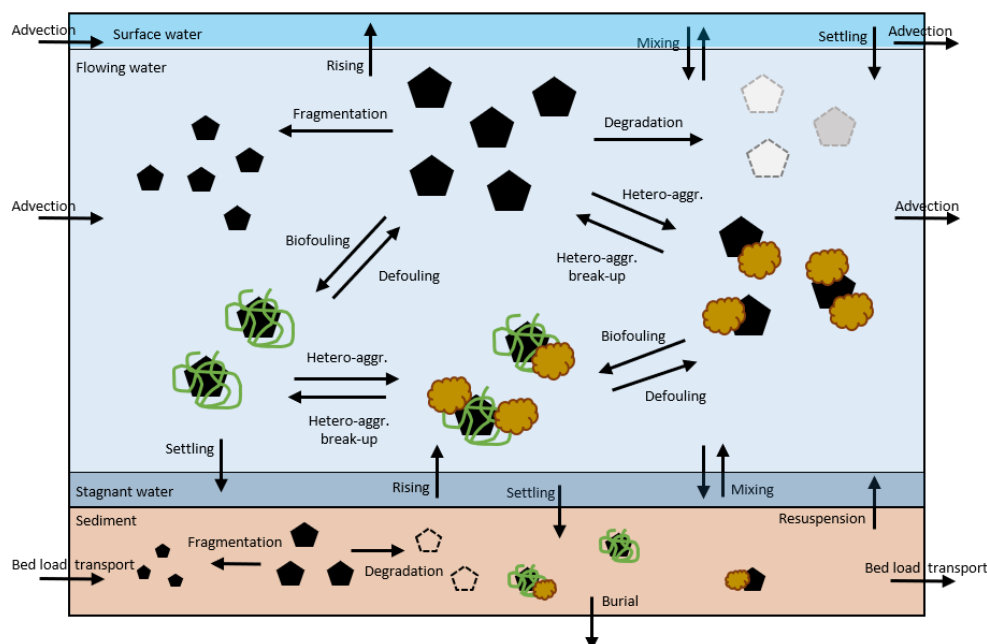


Figure 1. Schematic representation of the Full Multi model unit cell and the fate and transport processes modelled in the water (applicable to surface, flowing and stagnant water) and sediment compartments. Black pentagons represent plastic particles, brown clouds are SPM and green scribbles are biofilm.

In the generic river system described in the default parameterization, unit cells are connected in series by a unidirectional flow of water in the “flowing water” and “surface water” compartments, as well as bed load transport in the “sediment” compartments. To describe a specific river system, connections between unit cells can be added to describe tributaries to a main river channel. Each unit cell in a modeled system can be individually parameterised to describe the geographical and geochemical features of the water body, and their dimensioning will determine the spatial resolution of the model (Table 1).

2.1.2. Description of plastic particles

The plastic particles in the Full-Multi framework represented as a distribution of particles via discrete size classes and described by input parameters specifying density and shape (Table 1). The default parameterization of the model framework assumes five size classes (i.e. 0.1, 1, 10, 100 and 1000 μm particles), which represents a compromise between computational time/power requirements and resolution of plastic particles at a range of sizes.

The plastics can take on four different speciation forms: pristine, heteroaggregated, biofouled, and biofouled & heteroaggregated. While for the mass balance accounting the particles remain in their originally assigned size class upon speciation (i.e. each particle species is tracked within the size class of the parent pristine particle), effective changes in particles size and density are calculated for each species and accounted for in the calculation of fate processes.

For heteroaggregated and biofouled plastic particles, the effective size and density are calculated based on the equations shown in Table S1, to account for the impact of added volume and different density from SPM and biofilm. For the biofouled particle the calculations are based on a model study by Kooi et al. (2017), where the biofilm layer was assumed to have a thickness of 5 μm and a density of 1388 kg/m^3 . For the heteroaggregated species the SPM were assumed to have an spherical shape, a diameter of 0.5 μm and a density of 2000 kg/m^3 (Praetorius et al. 2012).

2.1.1. Fate processes

For each size class of plastic particles in water compartments, the Full Multi model simulates transformation of the particles between the four different microplastic species (i.e. heteroaggregation, aggregate break-up, biofouling and defouling), fragmentation into the next smallest size class, chemical degradation that removes plastic from the system, transport between compartments within a unit cell by settling, rising, mixing, and transport between unit cells by advection (Figure 1). In sediment compartments the modeled fate processes are fragmentation, degradation, burial into deep, inaccessible sediments, resuspension to the adjacent water compartment within the unit cell, and transport along the river between unit cells via bedload transport (Figure 1). The formulation of each of the processes included in the default parameterization of the Full Multi is based on a review of the literature, is described in more detail below and the equations are presented in Table S2.

The fate processes in the Full Multi framework can be broadly divided into three categories: *Interaction* with natural entities, *transformation* and *transport* between different compartments.

Interaction processes (heteroaggregation, breakup and biofouling)

Heteroaggregation, the aggregation of plastic particles with natural SPM, is modelled following classical colloid theory, as discussed in Praetorius et al. 2012, as a pseudo-first order process (Table S2). The rate constant for this process depends on the collision frequency between the two types of particles, the concentration of SPM present in the system and the attachment efficiency for heteroaggregation ($\alpha_{het-agg}$), describing the probability of heteroaggregate formation upon collision (Praetorius et al. 2020). $\alpha_{het-agg}$ describes the degree of favourable interaction between plastics and SPM and is influenced by the respective surface characteristics of the colliding particles as well as the water chemistry. In the default parameterization of the Full Multi model it is hypothesized that biofilm increases the attachment efficiency of a plastic particle (Besseling et al. 2017), reflected in two times higher values of $\alpha_{het-agg}$ for biofouled plastic particles compared to the pristine form. Breakup of plastic particle-SPM heteroaggregates is formulated in the Full Multi as being proportional to the rate

of heteroaggregation (Table S2). While experimental data are still very limited on the kinetics of heteroaggregate breakup, it is likely that this process is size dependent and therefore consideration of the size factor is suggested as future implementation in the model. The processes of heteroaggregation and breakup of heteroaggregates are included only in the water compartments of the current implementation of the framework as depicted in Figure 1.

Homoaggregation of plastic particles with themselves is not included in the current Full Multi version. Due to high dilution of plastic particles in the environment compared to naturally occurring SPM, homoaggregation is assumed negligible and does not justify the additional computational effort of including a second-order process in the model framework.

Biofouling is the process where organisms colonise the surface of submerged plastic particles and form a biofilm surface (Rummel et al. 2017). In the Full Multi framework biofouling is represented as a first-order kinetic process characterized by a characteristic time for biofilm to grow on the surface of the plastic particle ($t_{biof-growth}$). The default parameterization of the Full Multi framework considers biofilm growth on pristine and heteroaggregated particles that are present in water compartments and assumes that the time for biofilm growth varies with depth, following the hypothesis that biofouling occurs at slower rates in deeper waters due to reduced light limiting the growth of the biofilm organisms (Kooi et al. 2017). Hence, biofouling is fastest in the surface water compartment. Future applications of the model could also consider plastic additives present in the modelled particles as influencing the rate of biofouling (Nelson, Reddy, and Ward 2021) as well as different growth rates as a function of temperature, sunlight and water composition.

Defouling, the disintegration of the biofilm layer, can occur due to light limitation, grazing, or dissolution of carbonates in acid waters (Kooi et al. 2017). In the Full Multi framework defouling is represented as a first-order kinetic process characterized by a biofilm degradation time ($t_{biof-degrade}$). Despite being a potentially relevant fate process, the rate constant for defouling is assumed to be zero in all compartments in the current formulation of the Full Multi due to lack of data regarding biofilm degradation times.

Transformation processes (fragmentation and degradation)

Polymer degradation by biotic and/or abiotic processes is represented as a first-order degradation process based on estimated half-lives for degradation (t_{half}) (Table S2). For many plastic types, polymer degradation is expected to be a slow process (Ward and Reddy 2020), and degradation rates may be negligible compared to other processes in many systems. However, biodegradable polymers might have shorter degradation times and therefore this process is implemented in the framework. Currently, degradation is represented as complete

mineralization, but it would be possible to consider the formation of degradation intermediates and their fate in future model implementations.

Fragmentation of plastic particles in the Full Multi is modeled as a size-dependent process based on an estimated rate constant (k_{frag_gen}) for fragmentation of pristine particles in the largest (1000 μm) size class in flowing water. In the default parameterization, we assume fragmentation of pristine 1000 μm particles occurs on a 1-year timescale and set $k_{frag_gen} = 1/(1 \text{ year}) = 3.2 \times 10^{-8} \text{ s}^{-1}$. Fragmentation rate constants for all size classes of pristine particles are then calculated by scaling k_{frag_gen} assuming fragmentation occurs more slowly for smaller particles in proportion to the ratio of diameters. “Explosive” fractionation is assumed such that fragmentation produces a number of smaller particles calculated by dividing the volume of particles in the parent size class by the volume of particles in the daughter size class (Table S2). In the default formulation of the Full Multi, fragmentation is assumed to occur unidirectionally from larger to consecutively smaller size fractions only. Thus, for example, particles in the 1000 μm size class fragment into the 100 μm size class only. Fragmentation of plastic particles in the environment is driven by diverse factors such as UV radiation, physical stress induced by water turbulence and wind, and biodegradation (Min et al. 2020). In the default formulation of the Full Multi, fragmentation rates in surface water where UV radiation and turbulence are strongest, are assumed to be ten times higher than in the other water compartments. Fragmentation of heteroaggregated particles is assumed negligible in the default model formulation and biofouled particles are assumed to fragment at half the rate of the corresponding pristine plastic particle due to shielding of the particle's surface from UV radiation and physical stress.

Transport processes (advection, bed-load transport, burial, resuspension, settling, rising, mixing)

Advective transport of the plastic particles in the moving water compartments, horizontal transport in the sediment bed, vertical mixing of bulk water, burial into deep sediment and resuspension into stagnant water are modelled following the same assumptions and process formulations as in the model developed by Praetorius et al., 2012 describing the fate and transport of titanium dioxide nanoparticles in the Rhine River (Table S2).

First order rate constants for settling (or rising) of plastic particles are estimated based on the depth of the compartment of study and the value of settling (or rising) velocity of the plastic particle calculated using Stokes' law for theoretical settling velocities of a perfect sphere in a fluid with laminar flow (Praetorius et al., 2012) (Table S2). Settling and rising are mutually exclusive, and whether a particle settles or rises is determined by the density difference between the plastic particle and water. Limitations to this process description have been

identified in the literature and involve overestimation of settling velocities of large, low density particles, and underestimation of the influence of particle shape (Waldschläger and Schüttrumpf 2019; Kowalski et al. 2016). Other settling formulations can be implemented in the Full Multi framework by the user if desired.

2.1.3. Mass balance model equations

The mass balance equations for each particle species in each size class form a system of coupled first-order ordinary differential equations (ODEs) (eq.1.) that are functions of species- and size-specific particle number of plastics in each compartment of the model domain and of time. By default, concentrations (eq.2.) are expressed as number of plastic particles per volume in the water compartments and per dry weight mass in the sediment compartment by converting the volume of sediment into mass using a typical dry sediment bulk density 1.3 g/cm³ (Sekellick et al. 2013). The model allows interconversion between particle number and mass concentration by using the final density and parent size of the particle being evaluated (eq. 3).

$$\begin{aligned} \frac{dN_{Comp-Cell}^{F,i}}{dt} = & q_{Comp-Cell}^{F,i} - k_{loss}^{F,i} \times N_{Comp-Cell}^{F,i}(t) + \sum_{j=1}^{n_i^F} k_{transf}^{Fj,i-F,i} \times N_{Comp-Cell}^{Fj,i}(t) \\ & + \sum_{y=1}^{Comp} k_{transport}^{F,i} \times N_{y-n}^{F,i}(t) \end{aligned} \quad eq. 1.$$

$$C_{Comp-Cell}^{F,i} = \frac{N_{Comp-Cell}^{F,i}}{V_{Comp-Cell}} \quad eq.2.$$

$$C_{Comp-Cell}^{F,i} (mg \cdot m^{-3}) = C_{Comp-Cell}^{F,i} (num \cdot m^{-3}) \times V^{F,i} \times d^{F,i} \quad eq.3.$$

for $i = 1, \dots, n_{sizes}^F$ and $n = 1, \dots, n_{Model\ Cells}$

where F represents the microplastic speciation form (i.e. pristine, heteroaggregated, biofouled or biofouled & heteroaggregated), i the plastic particle size class, Comp the cell compartment

(i.e. surface water, flowing water, stagnant water and sediment) and Cell the specific model unit cell. $q_{Comp-Cell}^{F,i}$ refers to the input flow of plastic particles of form F and size class i , into the compartment and cell specified in particles per minute and $V_{Comp-Cell}$ is the volume of the compartment within the modelled cell. $N_{Comp-Cell}^{F,i}(t)$ is the number of particles of form F and size class i present in the compartment and cell specified and $k_{loss}^{F,i}$, $k_{transf}^{Fj,i-F,i}$ and $k_{transport}^{F,i}$ represent the rate constants for irreversible loss processes (which include degradation, fractionation from the smallest size class, burial and advection out of the system), the transformation rate constant from any other MP form j and size class i (i.e. heteroaggregation, break-up, biofouling, defouling, and fractionation) and the transport rate constant of the same plastic particle form and size class from the different compartments and/or unit cell, in s^{-1} respectively. $V^{F,i}$ represents the volume of the particle form F of size i and $d^{F,i}$ its density.

The set of ODEs arranged in matrix form (eq.4.) is solved in Python with the Scipy.integrate package using the function ODEINT.

$$\frac{dN}{dt} = N(t) \times M_{FullMulti} + Q_{input} \quad \text{eq.4.}$$

Where the vector $N(t)$ contains the particle numbers of the different plastic particle forms in different size classes for all compartments in the model. The matrix $M_{FullMulti}$ contains the rate constants of the mass balance equation eq.1 and Q_{input} is the emission vector.

2.2. Model parameterization

The Full Multi framework requires parameters to define the characteristics of the plastic particles, the fate process descriptors, the properties of the modelled system and the connectivity between model unit cells. These input parameters are specified in four input files, whose content is summarised in Table 1.

Table 1. List of input files and parameters required to parameterise the Full Multi model

Input file name	Information type	Parameters
-----------------	------------------	------------

MiroplasticsSizeClass.txt	Plastic particles characteristics	<ul style="list-style-type: none"> - Density (kg/m³) - Shape (i.e. sphere, fibre) - Diameter (µm) - Length a, b and c (for non- spherical particles) (l_a, l_b and l_c, in µm)
compartmentsGenericRiverSec_prop.txt	Cell dimensions and properties	<ul style="list-style-type: none"> - Depth, length and width (h, l and w in m) - Volume (V, in m³) - Shear rate (G, in s⁻¹) - Temperature (T, in K) - Flow velocity (v_{Flow}, in m/s) - Concentration of SPM (C_{SPM}, in mg/L)
process_paramRiver.txt	Fate process parameters	<ul style="list-style-type: none"> - Attachment efficiency ($\alpha_{het-agg}$) - Degradation half-life times (t_{half}, in days) - Timescale for fragmentation of the 1000 µm size fraction (t_{frag_gen}, in days) - Time of biofilm growth ($t_{biof-growth}$, in days)
flow_connectivity.csv	Connectivity between model cells regarding flow advection	<ul style="list-style-type: none"> -Discharge (q, in m³/h) -Region_I (cell of discharging inflow) -Region_J (cell of receiving inflow)

Emission scenarios also must be specified to define the Q_{input} vector and drive the model calculations. Emissions generally describe the time-variable input flow of plastic particles per minute, but they may also be specified as a pulse or constant emission flow rate. The location or locations where the emissions enter the model domain (i.e. the specific compartments and unit cells receiving emissions) must also be specified. The species and size class of plastic emitted into the system and the simulated time duration and target timestep for the ODE solver are also required inputs.

For the parameterisation of the different microplastic fate and transport processes included in the model a series of assumptions about how, when and where the different processes take place in the modelled system are required, and are documented in section 2.1.1 and Table S3.

Different degrees of confidence in the formulation of the processes (Table S2) or in the selection of the input parameters (Table S3) are highlighted, where those with low confidence levels correspond to processes where parameters are missing or highly uncertain and/or where process descriptions are based on assumptions that require critical evaluation by further research.

While particle shape is been included as a model input, the fate processes included in the current model version are only parameterised for spherically shaped particles. However, fibre process formulations are previewed for implementation.

3. ILLUSTRATIVE APPLICATION FOR A GENERIC RIVER

We illustrate the Full Multi framework by application to describe the fate and transport of plastic particles with a range of densities in a generic river system.

3.1. Framework configuration and parameterization

Our generic river system configuration of the Full Multi framework links model unit cells illustrated in Figure 1 with uni-directional water flow in the surface water and flowing water compartments, and with bedload transport of sediments (Figure 2).

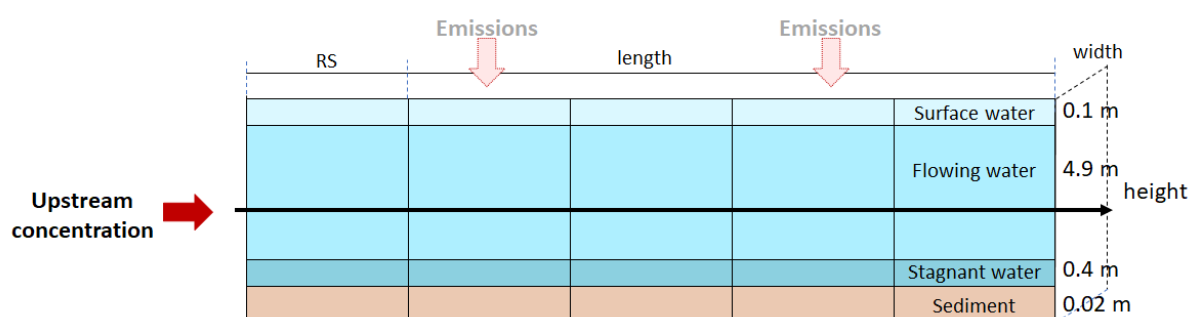


Figure 2. Schematic representation of the horizontal profile of the generic river model parameterization of the Full Multi framework in the longitudinal dimension showing all compartments and its dimensioning.

The modeled generic river is 1000 km long, and is subdivided into 20 unit cells with identical dimensions (50 km length, 80 m width and 5.42 m total depth) and with a water flow velocity of 1.3 m/s in the surface water and flowing water compartments (Figure 2). The unit cell structure, dimensions and flow velocity were inspired by the model for the Rhine river by Praetorius et al. (2012).

The process descriptions for plastic fate in the generic river system are parameterised according to the assumptions described in section 2.1.1 and are summarised in Table S3. In many cases these parameterizations and process descriptions are provisional and, according to our flexible and open-source modeling approach, they can be modified in future applications of the model as needed for scenario analysis or as new research emerges.

3.2. Scenario analysis for plastic with a range of densities

As an illustrative application of the model framework, we modeled a low density, buoyant plastic, assumed to be polyethylene (PE, $d=980\text{kg/m}^3$), a near-neutrally buoyant plastic, assumed to be polyamide (PA, $d=999\text{kg/m}^3$), and a high-density plastic, assumed to be polyvinyl chloride (PVC, $d=1580\text{kg/m}^3$). For each of these plastic types we simulated a constant emission of 100 pristine plastic particles per minute in the $1000\text{ }\mu\text{m}$ size class into the flowing water compartment of the first (i.e., the furthest up-stream) unit cell of the generic river. The model was run to simulate 365 days with a target timestep of 1 hour. After the model run information about the speciation of plastic particles, their dynamic exchange between the three water layers and sediment, and fragmentation into the five size classes (i.e. 0.1, 1, 10, 100 and $1000\text{ }\mu\text{m}$) is produced as output in the form of concentration values of each plastic species in each size class in each compartment in each unit cell of the river over time.

3.3. Results and discussion

3.3.1. Modeled concentrations after 1-year simulation time

Figures 3, 4 and 5 show the species and size class specific concentrations of plastic particles in our generic river system after one year of simulation of constant emission of PE, PA and PVC to the flowing water of the furthest up-stream unit cell of the model, respectively. Results are presented as number concentrations of plastic particles per m^3 in the water compartments, and per gram of sediment for the sediment compartment.

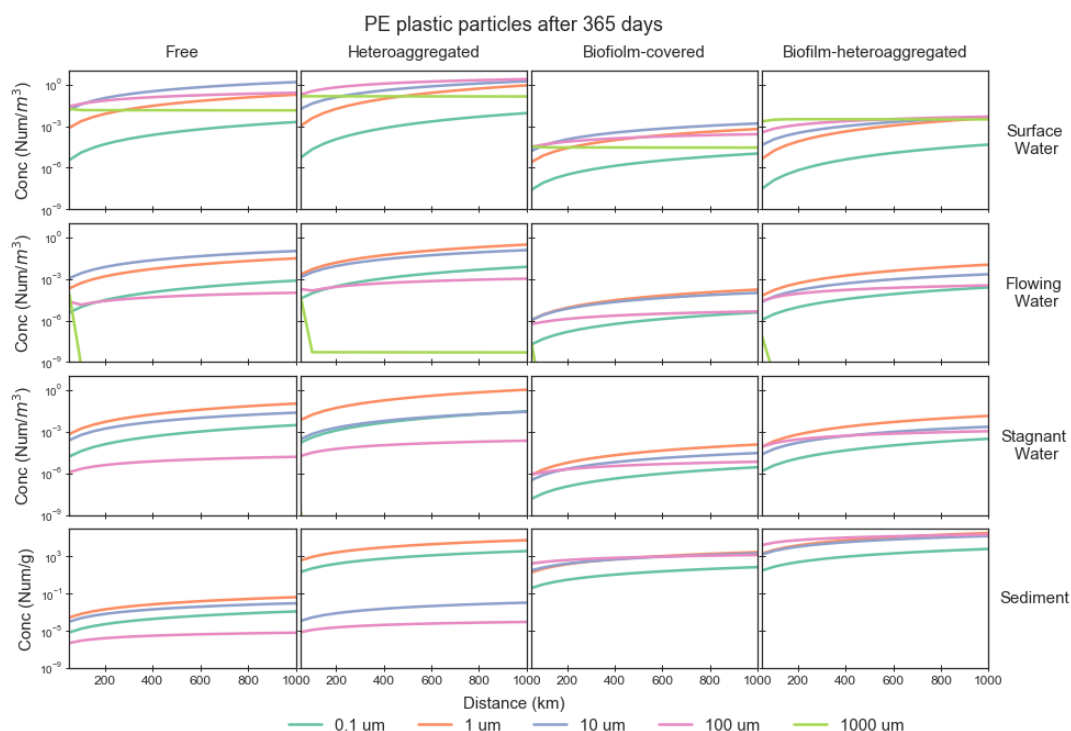


Figure 3. Concentration of the different forms of PE plastic particles (columns) in each compartment of the generic river system (rows) and for each size fraction (in different coloured lines) from upstream to downstream of the river. The concentration of particles in the water compartments is given in number of particles per m^3 and in sediment in number of particles per g of sediment.

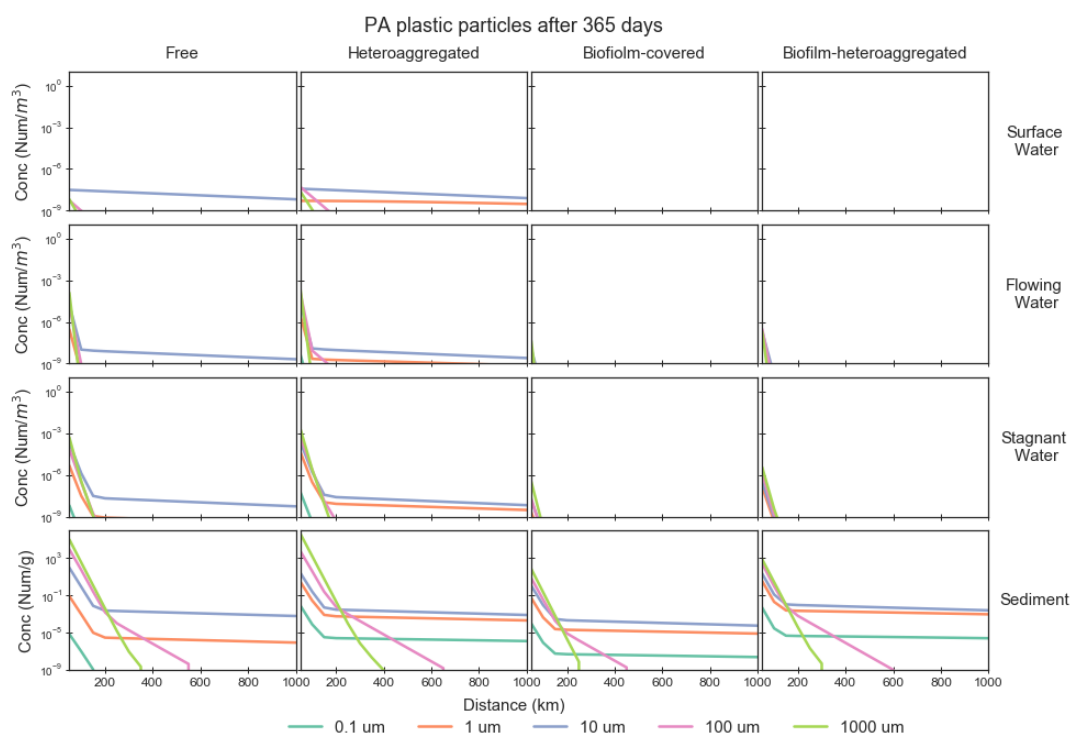


Figure 4. Concentration of the different forms of PA plastic particles (columns) in each compartment of the generic river system (rows) and for each size fraction (in different coloured lines) from upstream to

downstream of the river. The concentration of particles in the water compartments is given in number of particles per m³ and in sediment in number of particles per g of sediment.

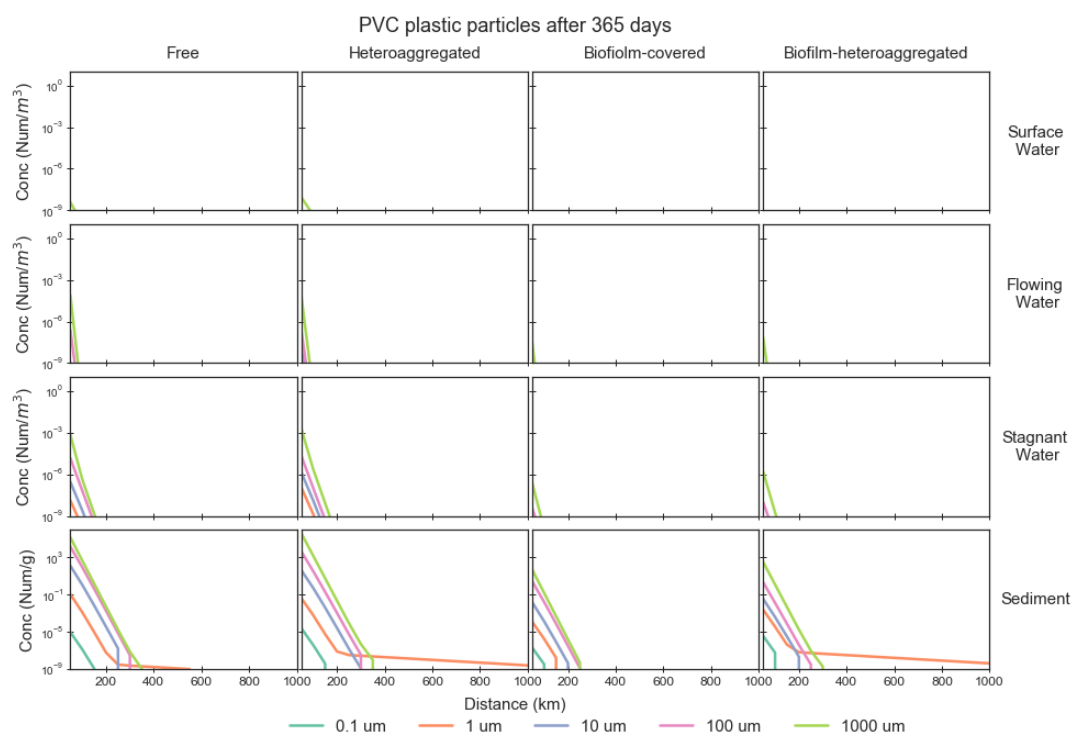


Figure 5. Concentration of the different forms of PVC plastic particles (columns) in each compartment of the generic river system (rows) and for each size fraction (in different coloured lines) from upstream to downstream of the river. The concentration of particles in the water compartments is given in number of particles per m³ and in sediment in number of particles per g of sediment.

From Figures 3, 4 and 5, we observe that, according to our model configuration and parameterization, the distribution of plastic particles between the different compartments along the whole river system differ strongly as a function of particle density and size. The buoyant low-density PE particles that remain in pristine form or are heteroaggregated are mainly found in the surface water and flowing water compartments. However, a fraction of their heteroaggregated and/or biofouled forms settle down to the sediment. The near-neutrally buoyant pristine particles of PA settle into the sediment compartment much more efficiently compared to PE regardless of aggregation state. However, some PA particles remain in the water compartments even far downstream in the river. Finally, all species of the high-density PVC particles are subject to sedimentation and burial into the deep sediment of the river, with only very low concentrations of the smallest size fractions being distributed downriver in the sediment compartment.

3.3.2. Comparing competing processes as half-life times

Since all processes in the model are described using first-order kinetics, they can be compared directly to each other. To facilitate comparison, we calculated half-life times for each process in each compartment of the model as $\ln 2/k_{\text{process}}$, where k_{process} is the process-specific rate constant in s^{-1} . The half-life time represents the time required for a particle's concentration to decrease to half its initial value due to the process in question only. Fate processes with the shortest half-life times are the fastest processes, and will be the dominant process pathways that plastic particles will follow in the modelled compartment.

Figures 6, 7 and 8 show process half-life times for each plastic particle species and size class for the three different plastic types. Green values correspond to short half-life times of a few minutes to tens of hours (from lighter to darker green), while the blue colour represents longer half-life times ranging from days to months to years (from lighter to darker blue). Grey shading marks processes that do not take place for the particular compartment, plastic form or size fraction, as formulated in the model. These heatmaps provide a visualization of the competing fate and transport pathways for the different species and size fractions of the three plastic types in our simulated generic river system with our default model formulation and parameterization.

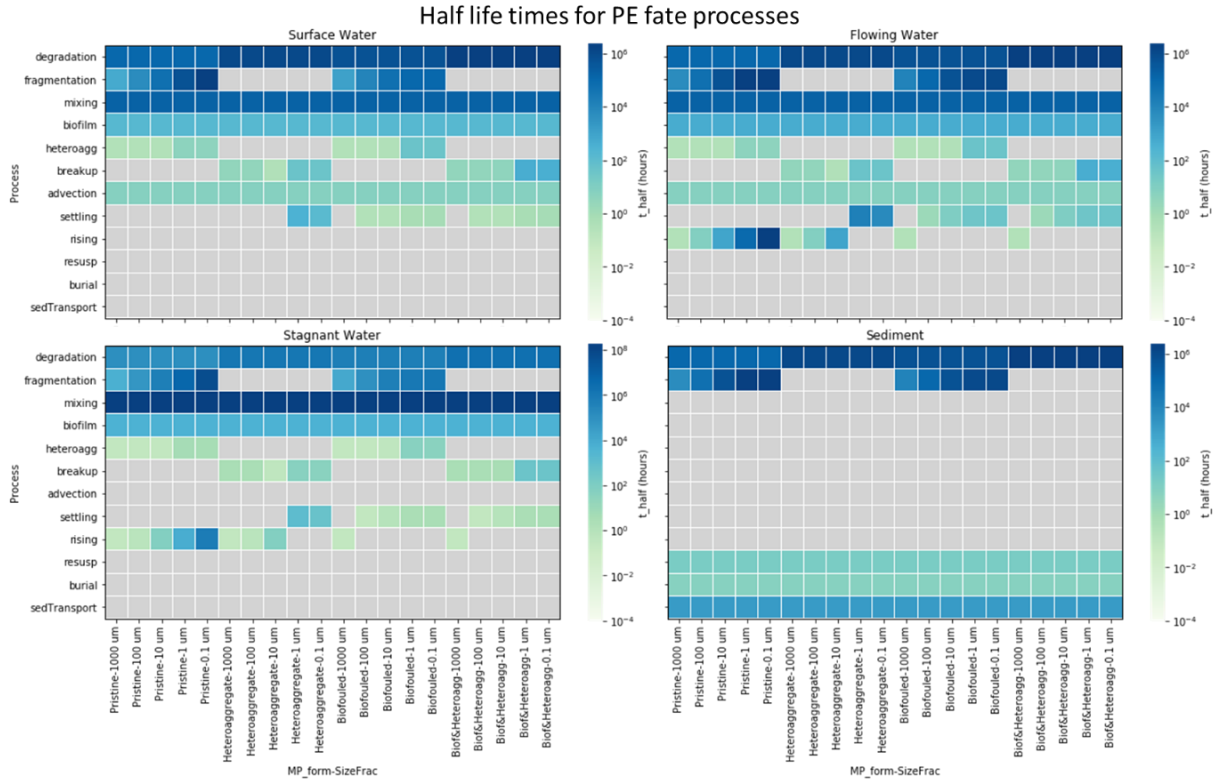


Figure 6. Heatmap of the fate and transport processes half-lifetimes (in hours) of PE microplastic particles in the simulated generic river system. Half-lifetimes of each process for each plastic species

and size fraction are indicated by a colour ramp from light green representing half-life times in minutes to dark blue half-life times of years.

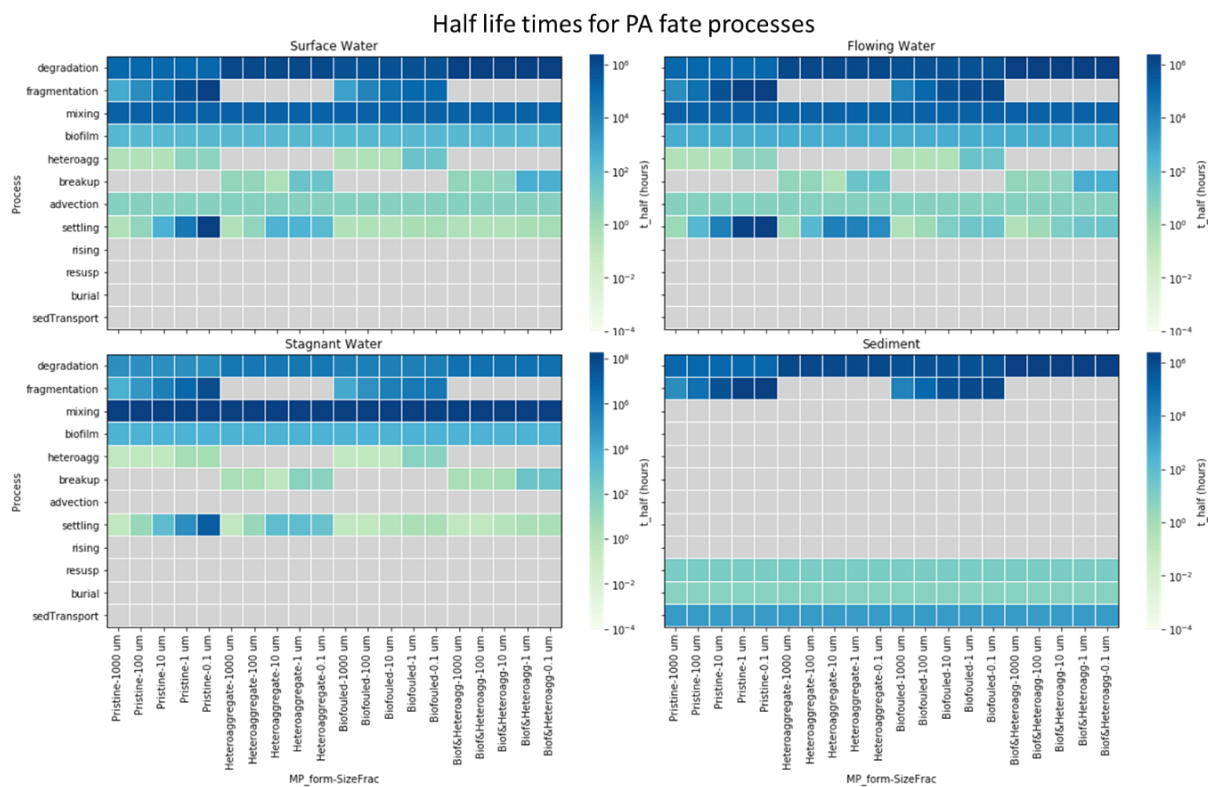


Figure 7. Heatmap of the fate and transport processes half-lifetimes (in hours) of PA microplastic particles in the simulated generic river system.

Settling and rising are mutually exclusive processes in the model; a plastic particle cannot simultaneously undergo settling and rising. Half-life times for settling or rising in water compartments, as formulated in the model, are a function of particle size and overall density, which is determined by the density of the plastic particle and the density of SPM for heteroaggregated particles and/or of biofilm for biofouled particles (Table S1). The density of water is specified as density of 998 kg/m³ in the default parameterization. Thus, pristine PE particles have lower density than water and rise rather than settle in the flowing and stagnant water compartments (Figure 6), while the pristine forms of PA and PVC settle (Figures 7 and 8). Small particles of low density PE that have been colonized by biofilm or heteroaggregated with particulate organic matter have higher bulk density than water (as described in table S1) which leads to settling rather than rising (Figure 6). Settling half-life times for the low-density PE particles range from 30 minutes to a few hours for the smallest heteroaggregated particles and for the biofouled particles. For PVC and PA particles, on the other hand, settling half live times range from 30 minutes to a few hours for the largest particles (10 to 1000 µm), but increase to several months for the smallest PA particles and the smallest, non-biofouled PVC particles, due to higher drag forces. PE half-life times for rising, for those particles with lower density than water, vary from 30 minutes to several months depending on the size and particle form, and are fastest for the largest 1000 µm size fraction.

3.3.3 Model evaluation against field data

The generic river parameterization and constant emissions assumed in our illustrative example does not allow for evaluation of the model against absolute concentrations of plastic particles measured in a real river. However, a degree of evaluation of the model against field data is possible by comparing the modeled size distribution of plastic particles to field measurements. Kooi and Koelmans (2019) collected data from 11 studies that reported plastic particle concentrations in 10 or more size classes and fitted the relative abundance of particles as a function of size with power law regressions. Our modeled relative abundance of PE plastic particles in the three water compartments in the last (i.e. furthest downstream) unit cell of the generic river after 1 simulated year falls within the range of measurements of floating plastic (Figure 9), which provides a partial validation of the assumptions about fragmentation made in the model.

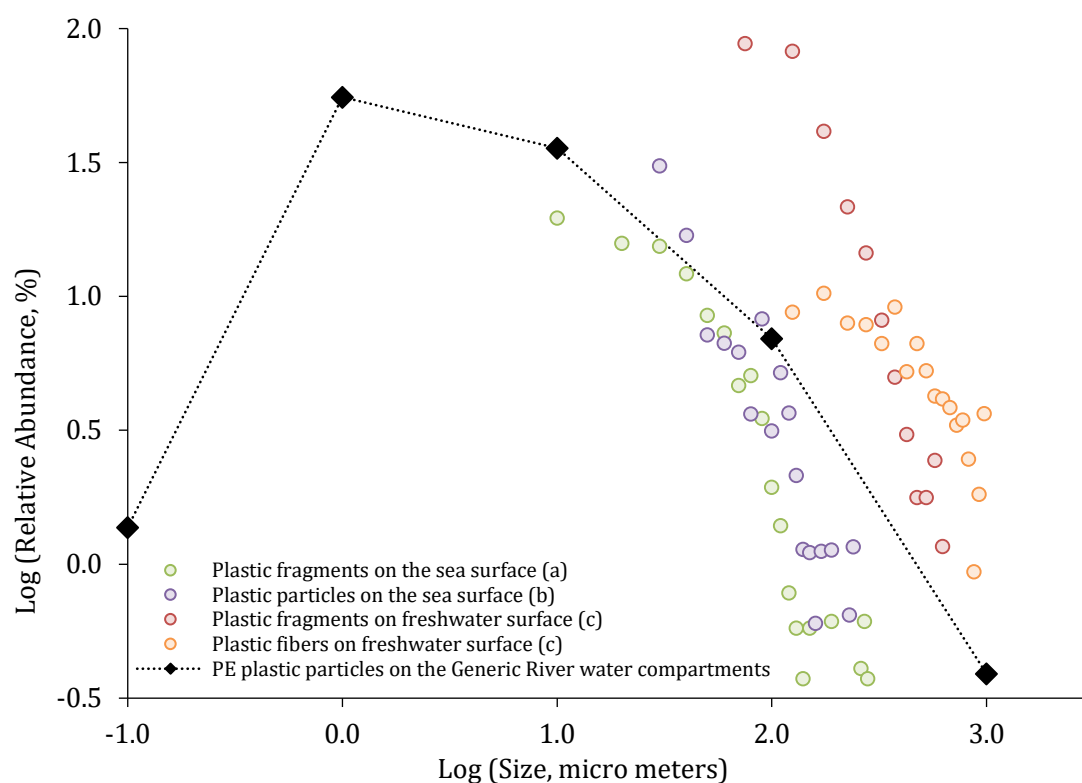


Figure 9. Relative plastic particle abundance for different particle sizes estimated by Kooi et al. (2019) from sea surface and freshwater surface samples ((a)Enders et al., 2015, (b)Erni-Cassola et al., 2017, (c) Eo et al., 2019) and from our model simulations in the generic river system for PE plastic particles.

In terms of distribution of the plastic particles within the different compartments of the generic river system, Table 2 summarises the model estimated particles distribution, integrated over all size ranges and species, as percentage of particles per compartment relative to the total number of particles in the system.

Table 2. Percentage of particles (in number of particles) per river section relative to the total amount of particles in the generic river after one-year simulation for PE, PA and PVC plastic particles.

	Surface Water (%)	Flowing Water (%)	Stagnant Water (%)	Sediment (%)
PE (980 kg/m ³)	21.12	66.82	11.48	0.58
PA (999 kg/m ³)	0.0	14.32	7.67	78.01
PVC (1580 kg/m ³)	0.0	4.36	6.23	89.41

These results are in line with results obtained from field studies where it was found that the higher density polymers prevailed in samples taken from river and marine sediments, while a larger percentage of buoyant polymers were found in surface water samples of fresh waters, effluents and to a lower extent, marine surface waters (Kooi et al. 2021).

4. CONCLUSIONS

We present a modeling framework to describe the fate of plastic particles in aquatic systems that describes multiple dimensions of particle characteristics (size and speciation) and that can be applied to diverse aquatic systems. We envision this framework as a tool to support hypothesis generation for process-level studies and data analysis, design of field measurement campaigns, scenario analysis and developing bounding exposure estimates for risk assessment.

The calculations for PE, PA and PVC in the generic river system presented in this paper can be replicated by prospective users of the framework by following tutorials in Jupyter notebooks on the models GitHub repository (https://github.com/Nano2PlastProject/TheFullMulti_RIVER). The full open-access model code is also available there and open for continued development.

Our evaluation of the modelled relative abundance of floating plastics in our generic scenario against field measurements provides a degree of confirmation that the fragmentation process descriptions in the model are reasonable. However additional performance evaluation and validation should be carried out before the model is used in risk assessment or decision support applications. An interesting feature of the model results illustrated in Figure 9 is the model's prediction of low relative abundance of 0.1 μm particles. In their review and meta-analysis of measurement data, Kooi and Koelmans (2019) reported that some datasets showed increasing particle concentrations with increasing size below 20 μm . However, they did not have confidence in this finding due to the methodological challenges of quantifying small plastic particles, and they suggested a practical detection limit of 20 μm . Our generic river modeling with the current process descriptions and parameterization predicts a maximum in relative abundance of floating plastic particles at around 1 μm diameter. That prediction is an example of how the model framework can be used for hypothesis generation to inspire further plastic pollution research.

5. ACKNOWLEDGMENTS

Development of The Full Multi was funded by the European Chemical Industry Council (CEFIC) through the Long-Range Research Initiative (LRI) project ECO48 - NANO2PLAST: Extending nanoparticle models to open-source models of the fate and transport of microplastic in aquatic systems.

6. REFERENCES

Arp, Hans Peter H., Dana Kühnel, Christoph Rummel, Matthew MacLeod, Annegret Potthoff, Sophia Reichelt, Elisa Rojo-Nieto, et al. 2021. 'Weathering Plastics as a Planetary

- Boundary Threat: Exposure, Fate, and Hazards'. *Environmental Science & Technology*, May. <https://doi.org/10.1021/acs.est.1c01512>.
- Besseling, Ellen, Joris T. K. Quik, Muzhi Sun, and Albert A. Koelmans. 2017. 'Fate of Nano- and Microplastic in Freshwater Systems: A Modeling Study'. *Environmental Pollution* 220 (January): 540–48. <https://doi.org/10.1016/j.envpol.2016.10.001>.
- Dietrich, William E. 1982. 'Settling Velocity of Natural Particles'. *Water Resources Research* 18 (6): 1615–26. <https://doi.org/10.1029/WR018i006p01615>.
- Fazey, Francesca M. C., and Peter G. Ryan. 2016. 'Biofouling on Buoyant Marine Plastics: An Experimental Study into the Effect of Size on Surface Longevity'. *Environmental Pollution* 210 (March): 354–60. <https://doi.org/10.1016/j.envpol.2016.01.026>.
- Garner, Kendra L., Sangwon Suh, and Arturo A. Keller. 2017. 'Assessing the Risk of Engineered Nanomaterials in the Environment: Development and Application of the NanoFate Model'. *Environmental Science & Technology* 51 (10): 5541–51. <https://doi.org/10.1021/acs.est.6b05279>.
- González-Fernández, Daniel, Andrés Cózar, Georg Hanke, Josué Viejo, Carmen Morales-Caselles, Rigers Bakiu, Damià Barceló, et al. 2021. 'Floating Macrolitter Leaked from Europe into the Ocean'. *Nature Sustainability* 4 (6): 474–83. <https://doi.org/10.1038/s41893-021-00722-6>.
- Hoellein, Timothy J., Ariel J. Shogren, Jennifer L. Tank, Paul Risteca, and John J. Kelly. 2019. 'Microplastic Deposition Velocity in Streams Follows Patterns for Naturally Occurring Allochthonous Particles'. *Scientific Reports* 9 (1): 3740. <https://doi.org/10.1038/s41598-019-40126-3>.
- Horton, Alice A., Alexander Walton, David J. Spurgeon, Elma Lahive, and Claus Svendsen. 2017. 'Microplastics in Freshwater and Terrestrial Environments: Evaluating the Current Understanding to Identify the Knowledge Gaps and Future Research Priorities'. *Science of The Total Environment* 586 (May): 127–41. <https://doi.org/10.1016/j.scitotenv.2017.01.190>.
- Hüffer, Thorsten, Antonia Praetorius, Stephan Wagner, Frank von der Kammer, and Thilo Hofmann. 2017. 'Microplastic Exposure Assessment in Aquatic Environments: Learning from Similarities and Differences to Engineered Nanoparticles'. *Environmental Science & Technology* 51 (5): 2499–2507. <https://doi.org/10.1021/acs.est.6b04054>.
- Jahnke, Annika, Hans Peter H. Arp, Beate I. Escher, Berit Gewert, Elena Gorokhova, Dana Kühnel, Martin Ogonowski, et al. 2017. 'Reducing Uncertainty and Confronting Ignorance about the Possible Impacts of Weathering Plastic in the Marine Environment'. *Environmental Science & Technology Letters* 4 (3): 85–90. <https://doi.org/10.1021/acs.estlett.7b00008>.
- Kaiser, David, Nicole Kowalski, and Joanna J. Waniek. 2017. 'Effects of Biofouling on the Sinking Behavior of Microplastics'. *Environmental Research Letters* 12 (12): 124003. <https://doi.org/10.1088/1748-9326/aa8e8b>.
- Koelmans, Albert A., Merel Kooi, Kara Lavender Law, and Erik van Seville. 2017. 'All Is Not Lost: Deriving a Top-down Mass Budget of Plastic at Sea'. *Environmental Research Letters* 12 (11): 114028. <https://doi.org/10.1088/1748-9326/aa9500>.
- Kooi, Merel, and Albert A. Koelmans. 2019. 'Simplifying Microplastic via Continuous Probability Distributions for Size, Shape, and Density'. *Environmental Science & Technology Letters* 6 (9): 551–57. <https://doi.org/10.1021/acs.estlett.9b00379>.
- Kooi, Merel, Egbert H. van Nes, Marten Scheffer, and Albert A. Koelmans. 2017. 'Ups and Downs in the Ocean: Effects of Biofouling on Vertical Transport of Microplastics'. *Environmental Science & Technology* 51 (14): 7963–71. <https://doi.org/10.1021/acs.est.6b04702>.
- Kooi, Merel, Sebastian Primpke, Svenja M. Mintenig, Claudia Lorenz, Gunnar Gerdt, and Albert A. Koelmans. 2021. 'Characterizing the Multidimensionality of Microplastics across Environmental Compartments'. *Water Research*, July, 117429. <https://doi.org/10.1016/j.watres.2021.117429>.

- Kowalski, Nicole, Aurelia M. Reichardt, and Joanna J. Waniek. 2016. 'Sinking Rates of Microplastics and Potential Implications of Their Alteration by Physical, Biological, and Chemical Factors'. *Marine Pollution Bulletin* 109 (1): 310–19. <https://doi.org/10.1016/j.marpolbul.2016.05.064>.
- Lebreton, L. C. -M., S. D. Greer, and J. C. Borrero. 2012. 'Numerical Modelling of Floating Debris in the World's Oceans'. *Marine Pollution Bulletin* 64 (3): 653–61. <https://doi.org/10.1016/j.marpolbul.2011.10.027>.
- Lebreton, Laurent C. M., Joost van der Zwet, Jan-Willem Damsteeg, Boyan Slat, Anthony Andrady, and Julia Reisser. 2017. 'River Plastic Emissions to the World's Oceans'. *Nature Communications* 8 (1): 15611. <https://doi.org/10.1038/ncomms15611>.
- Liu, Haoyang Haven, and Yoram Cohen. 2014. 'Multimedia Environmental Distribution of Engineered Nanomaterials'. *Environmental Science & Technology* 48 (6): 3281–92. <https://doi.org/10.1021/es405132z>.
- Liubartseva, S., G. Coppini, R. Lecci, and S. Creti. 2016. 'Regional Approach to Modeling the Transport of Floating Plastic Debris in the Adriatic Sea'. *Marine Pollution Bulletin* 103 (1): 115–27. <https://doi.org/10.1016/j.marpolbul.2015.12.031>.
- Lobelle, Delphine, Merel Kooi, Albert A. Koelmans, Charlotte Laufkötter, Cleo E. Jongedijk, Christian Kehl, and Erik van Sebille. 2021. 'Global Modeled Sinking Characteristics of Biofouled Microplastic'. *Journal of Geophysical Research: Oceans* 126 (4): e2020JC017098. <https://doi.org/10.1029/2020JC017098>.
- MacLeod, Matthew, Hans Peter H. Arp, Mine B. Tekman, and Annika Jahnke. 2021. 'The Global Threat from Plastic Pollution'. *Science* 373 (6550): 61–65. <https://doi.org/10.1126/science.abg5433>.
- MacLeod, Matthew, Martin Scheringer, Thomas E. McKone, and Konrad Hungerbühler. 2010. 'The State of Multimedia Mass-Balance Modeling in Environmental Science and Decision-Making'. *Environmental Science & Technology* 44 (22): 8360–64. <https://doi.org/10.1021/es100968w>.
- Meesters, Johannes A. J., Albert A. Koelmans, Joris T. K. Quik, A. Jan Hendriks, and Dik van de Meent. 2014. 'Multimedia Modeling of Engineered Nanoparticles with SimpleBox4nano: Model Definition and Evaluation'. *Environmental Science & Technology* 48 (10): 5726–36. <https://doi.org/10.1021/es500548h>.
- Min, Kyungjun, Joseph D. Cuiffi, and Robert T. Mathers. 2020. 'Ranking Environmental Degradation Trends of Plastic Marine Debris Based on Physical Properties and Molecular Structure'. *Nature Communications* 11 (1): 727. <https://doi.org/10.1038/s41467-020-14538-z>.
- Nelson, Taylor F., Christopher M. Reddy, and Collin P. Ward. 2021. 'Product Formulation Controls the Impact of Biofouling on Consumer Plastic Photochemical Fate in the Ocean'. *Environmental Science & Technology* 55 (13): 8898–8907. <https://doi.org/10.1021/acs.est.1c02079>.
- Peng, Licheng, Dongdong Fu, Huaiyuan Qi, Christopher Q. Lan, Huamei Yu, and Chengjun Ge. 2020. 'Micro- and Nano-Plastics in Marine Environment: Source, Distribution and Threats — A Review'. *Science of The Total Environment* 698 (January): 134254. <https://doi.org/10.1016/j.scitotenv.2019.134254>.
- Praetorius, Antonia, Elena Badetti, Andrea Brunelli, Arnaud Clavier, Julián Alberto Gallego-Urrea, Andreas Gondikas, Martin Hassellöv, et al. 2020. 'Strategies for Determining Heteroaggregation Attachment Efficiencies of Engineered Nanoparticles in Aquatic Environments'. *Environmental Science: Nano* 7 (2): 351–67. <https://doi.org/10.1039/C9EN01016E>.
- Praetorius, Antonia, Martin Scheringer, and Konrad Hungerbühler. 2012a. 'Development of Environmental Fate Models for Engineered Nanoparticles—A Case Study of TiO₂ Nanoparticles in the Rhine River'. *Environmental Science & Technology* 46 (12): 6705–13. <https://doi.org/10.1021/es204530n>.
- . 2012b. 'Development of Environmental Fate Models for Engineered Nanoparticles--a Case Study of TiO₂ Nanoparticles in the Rhine River'. *Environmental Science & Technology* 46 (12): 6705–13. <https://doi.org/10.1021/es204530n>.

- Praetorius, Antonia, Nathalie Tufenkji, Kai-Uwe Goss, Martin Scheringer, Frank von der Kammer, and Menachem Elimelech. 2014. 'The Road to Nowhere: Equilibrium Partition Coefficients for Nanoparticles'. *Environmental Science: Nano* 1 (4): 317–23. <https://doi.org/10.1039/C4EN00043A>.
- Rochman, Chelsea M., Cole Brookson, Jacqueline Bikker, Natasha Djuric, Arielle Earn, Kennedy Bucci, Samantha Athey, et al. 2019. 'Rethinking Microplastics as a Diverse Contaminant Suite'. *Environmental Toxicology and Chemistry* 38 (4): 703–11. <https://doi.org/10.1002/etc.4371>.
- Rummel, Christoph D., Annika Jahnke, Elena Gorokhova, Dana Kühnel, and Mechthild Schmitt-Jansen. 2017. 'Impacts of Biofilm Formation on the Fate and Potential Effects of Microplastic in the Aquatic Environment'. *Environmental Science & Technology Letters* 4 (7): 258–67. <https://doi.org/10.1021/acs.estlett.7b00164>.
- Sebille, Erik van, Chris Wilcox, Laurent Lebreton, Nikolai Maximenko, Britta Denise Hardesty, Jan A. van Franeker, Marcus Eriksen, David Siegel, Francois Galgani, and Kara Lavender Law. 2015. 'A Global Inventory of Small Floating Plastic Debris'. *Environmental Research Letters* 10 (12): 124006. <https://doi.org/10.1088/1748-9326/10/12/124006>.
- Sekellick, Andrew J., William S.L. Banks, and Michael K. Myers. 2013. 'Water Volume and Sediment Volume and Density in Lake Linganore between Boyers Mill Road Bridge and Bens Branch, Frederick County, Maryland, 2012'. USGS Numbered Series 2013–5082. *Water Volume and Sediment Volume and Density in Lake Linganore between Boyers Mill Road Bridge and Bens Branch, Frederick County, Maryland, 2012*. Vol. 2013–5082. Scientific Investigations Report. Reston, VA: U.S. Geological Survey. <https://doi.org/10.3133/sir20135082>.
- Semcesen, Patricia O., and Mathew G. Wells. 2021. 'Biofilm Growth on Buoyant Microplastics Leads to Changes in Settling Rates: Implications for Microplastic Retention in the Great Lakes'. *Marine Pollution Bulletin* 170 (September): 112573. <https://doi.org/10.1016/j.marpolbul.2021.112573>.
- Siegfried, Max, Albert A. Koelmans, Ellen Besseling, and Carolien Kroeze. 2017. 'Export of Microplastics from Land to Sea. A Modelling Approach'. *Water Research* 127 (December): 249–57. <https://doi.org/10.1016/j.watres.2017.10.011>.
- Unice, K. M., M. P. Weeber, M. M. Abramson, R. C. D. Reid, J. A. G. van Gils, A. A. Markus, A. D. Vethaak, and J. M. Panko. 2019. 'Characterizing Export of Land-Based Microplastics to the Estuary - Part II: Sensitivity Analysis of an Integrated Geospatial Microplastic Transport Modeling Assessment of Tire and Road Wear Particles'. *Science of The Total Environment* 646 (January): 1650–59. <https://doi.org/10.1016/j.scitotenv.2018.08.301>.
- Wagner, Martin, Christian Scherer, Diana Alvarez-Muñoz, Nicole Brennholt, Xavier Bourrain, Sebastian Buchinger, Elke Fries, et al. 2014. 'Microplastics in Freshwater Ecosystems: What We Know and What We Need to Know'. *Environmental Sciences Europe* 26 (1): 12. <https://doi.org/10.1186/s12302-014-0012-7>.
- Waldschläger, Kryss, and Holger Schüttrumpf. 2019. 'Effects of Particle Properties on the Settling and Rise Velocities of Microplastics in Freshwater under Laboratory Conditions'. *Environmental Science & Technology* 53 (4): 1958–66. <https://doi.org/10.1021/acs.est.8b06794>.
- Ward, Collin P., and Christopher M. Reddy. 2020. 'Opinion: We Need Better Data about the Environmental Persistence of Plastic Goods'. *Proceedings of the National Academy of Sciences* 117 (26): 14618–21. <https://doi.org/10.1073/pnas.2008009117>.
- Wijnen, Jikke van, Ad M. J. Ragas, and Carolien Kroeze. 2019. 'Modelling Global River Export of Microplastics to the Marine Environment: Sources and Future Trends'. *Science of The Total Environment* 673 (July): 392–401. <https://doi.org/10.1016/j.scitotenv.2019.04.078>.
- Ye, Song, and Anthony L. Andrady. 1991. 'Fouling of Floating Plastic Debris under Biscayne Bay Exposure Conditions'. *Marine Pollution Bulletin* 22 (12): 608–13. [https://doi.org/10.1016/0025-326X\(91\)90249-R](https://doi.org/10.1016/0025-326X(91)90249-R).

SUPPORTING INFORMATION

S1. Model Description

Table S1. Formulas used for the estimation of the size and density of the biofouled and heteroaggregated plastic particles adapted from Kooi et al. (2007). Being r_{PP} the plastic particle radius (m), ρ_{PP} the plastic particle density (kg/m³), T_{BF} the thickness of the biofilm layer (m), ρ_{BF} the density of the biofilm (kg/m³), V_{PP} the volume of plastic particle (m³), V_{SPM} the volume of SPM particle (m³) and ρ_{SPM} the density of SPM particle(kg/m³).

	Particle size (r_{PP})	Particle density (ρ_{PP})
Biofouled Particles (PP-BF)	$r_{PP-BF} = r_{PP} + T_{BF}$	$\rho_{PP-BF} = \frac{r_{PP}^3 \times \rho_{PP} + ((r_{PP} + T_{BF})^3 - r_{PP}^3) \times \rho_{BF}}{(r_{PP} + T_{BF})^3}$
Heteroaggregated particles (PP-SPM)	$r_{PP-SPM} = \sqrt[3]{\frac{3 \times (V_{PP} + V_{SPM})}{4 \times \pi}}$	$\rho_{PP-SPM} = \rho_{PP} \times \frac{V_{PP}}{V_{PP} + V_{SPM}} + \rho_{SPM} \times \frac{V_{SPM}}{V_{PP} + V_{SPM}}$

Table S2. Formulas used for the microplastics fate and transport processes included in the Full-Multi model framework. Colour related to level of confidence in the formulation (Green= high; Orange=medium; Red=low)

Fate process	Formula	Parameters	Reference
Degradation	$k_{deg} = \frac{\ln 2}{t_{half} \times 24 \times 60 \times 60}$	t_{half} : degradation half-life in days	Assumed first order kinetics
Fragmentation	$k_{frag} = k_{frag_gen} \times \frac{D_i}{D_{1000}}$ $k_{frag_gen} = \frac{1}{t_{frag_gen}}$ $V_{frag} = \frac{4}{3} \times \pi \times \left(\frac{D_{MP}/2}{10}\right)^3$	k_{frag_gen} : number of MP fragments formed per day D_i : diameter of particle i in μm t_{frag_gen} : timescale for fragmentation of the 1000 μm size fraction	D_{MP} acts as a factor relative to size, bigger MPs have faster fractionation rates.

	$N_{frag} = \frac{V_{MP}}{V_{frag}}$	N_{frag} : number of fragments formed V_{MP} : volume of the MP (μm^3) V_{frag} : volume of the fragment (μm^3)	
Advection	$k_{flow} = v_{flowRiver} \times \frac{A_{comp}}{V_{comp}}$	$v_{flowRiver}$: average flow velocity (ms^{-1}) A_{comp} : cross sectional area of the compartment (m^2) V_{comp} : volume of the compartment of moving water (m^3)	(Praetorius et al. 2012)
Biofouling	$k_{biof} = \frac{1}{(t_{biof-growth}/60)}$	$t_{biof-growth}$: time for the biofilm coverage to grow in minutes	Assumed first order kinetics
Defouling	$k_{defoul} = \frac{1}{(t_{biof-degrade}/60)}$	$t_{biof-degrade}$: time for the biofilm coverage to degrade in minutes	Assumed first order kinetics
Heteroaggregation	$k_{hetAgg} = \alpha_{het-agg} \times k_{coll} \times C_{SPM}$	$\alpha_{het-agg}$: heteroaggregation attachment efficiency C_{SPM} : SPM concentration (mg/L) k_{coll} : collisions rate constant (s^{-1})	(Praetorius et al. 2012; Praetorius et al. 2020)
Aggregate breakup	$k_{agg-breakup} = \frac{1}{10} k_{hetAgg}$	k_{hetAgg} : heteroaggregation rate constant (s^{-1})	
Settling	$k_{set} = \frac{v_{set}}{h_{comp}}$ $v_{set} = \frac{2}{9} \times \frac{(\rho_{MP} - \rho_{water})}{\mu_{water} \times r_{MP}^2} \times g$	v_{set} : settling velocity of the MP particle (m/s) ρ_{MP} : density of the MP (kg/m^3) μ_{water} : dynamic viscosity of water at 21C (kg/ms)	(Dietrich 1982; Praetorius et al. 2012)

		ρ_{water} : density of water at 21C (kg/m ³) g : gravitational acceleration on earth in (m/s ²) r_{MP} : radius of the MP particle (m) h_{comp} : compartment depth (m)	
Rising	$k_{rise} = -\frac{v_{set}}{h_{comp}}$	v_{set} : settling velocity of the MP particle (m/s) h_{comp} : compartment depth (m)	
Mixing	<p>For the surface water compartment:</p> $k_{mix} = 10^{-10} \times \frac{V_{flowingWater}}{V_{surfaceWater}}$ <p>For the stagnant water compartment:</p> $k_{mix} = 10^{-13} \times \frac{V_{flowingWater}}{V_{stagnantWater}}$ <p>No mixing assumed for the sediment compartment.</p>	$V_{flowingWater}$: volume of flowing water compartment (m ³) $V_{surfaceWater}$: volume of surface water compartment (m ³) $V_{stagnantWater}$: volume of stagnant water (m ³)	Assumed first order kinetics and normalised by volume of the compartment (Praetorius, Scheringer, and Hungerbühler 2012)
Resuspension	$k_{resusp} = \frac{2.3 \times 10^{-7}}{h_{comp}}$	h_{comp} : compartment depth (m)	(Praetorius, Scheringer, and Hungerbühler 2012)
Burial	$k_{burial} = \frac{5.6 \times 10^{-7}}{h_{comp}}$	h_{comp} : compartment depth (m)	(Praetorius, Scheringer, and Hungerbühler 2012)

Sediment transport	$k_{sed-trans} = \frac{v_{sed-transp}}{m_{sed}}$ $m_{sed} = (1 - p_{sed}) \times d_{sed} \times V_{sed}$	$v_{sed-transp}$: velocity of sediment transfer (kg/s) m_{sed} : mass of sediment (kg) p_{sed} : sediment porosity d_{sed} : sediment density (g/cm ³) V_{sed} : volume of sediment (m ³)	(Praetorius, Scheringer, and Hungerbühler 2012)
--------------------	--	--	---

S2. Model parameterization

Table S3. Selected values of fate process descriptors per river compartment and MP form. Being $\alpha_{het-agg}$ the heteroaggregation attachment efficiency, $t_{biof-growth}$ the time for the biofilm coverage to grow, t_{half} the degradation half-life of the MP particles, $t_{frag-gen}$ timescale for fragmentation of the 1000 μm size fraction and $t_{biof-degrade}$ the time required for the biofilm layer to degrade. Colour related to level of confidence in the parameterization (Green= high; Orange=medium; Red=low)

Compartment	MP- form	$\alpha_{het-agg}$	$t_{biof-growth}$ (days)	t_{half} (days)	$t_{frag-gen}$ (days)	$t_{biof-degrade}$ (days)
Surface Water	Pristine-MP	0.01*	10	5000	36.5	-
	Heteroagg-MP	-	10	50000	-	-
	Biofouled-MP	0.02*	10	25000	73.0	NAN
	Heteroagg-Biofouled-MP	-	10	100000	-	NAN
Flowing Water	Pristine-MP	0.01*	30	5000	356	-
	Heteroagg-MP	-	30	50000	-	-
	Biofouled-MP	0.02*	30	25000	730	NAN
	Heteroagg-Biofouled-MP	-	30	100000	-	NAN

Stagnant Water	Pristine-MP	0.01*	300	5000	365	-
	Heteroagg-MP	-	300	50000	-	-
	Biofouled-MP	0.02*	300	25000	730	NAN
	Heteroagg-Biofouled-MP	-	300	100000	-	NAN
Sediment top layer	Pristine-MP	-	-	5000	365	-
	Heteroagg-MP	-	-	50000	-	-
	Biofouled-MP	-	-	25000	730	NAN
	Heteroagg-Biofouled-MP	-	-	100000	-	NAN

*Besseling et al. (2017)